

# Isogeometric Shape Optimization of Multi-Tapered Coaxial Baluns Simulated by an Integral Equation Method

Boian Balouchev

Computational Electromagnetics  
Technische Universität Darmstadt  
Darmstadt, Germany  
boian.balouchev@stud.tu-darmstadt.de

Jürgen Dölz

Institute for Numerical Simulation  
University of Bonn  
Bonn, Germany  
doelz@ins.uni-bonn.de

Maximilian Nolte

Computational Electromagnetics  
Technische Universität Darmstadt  
Darmstadt, Germany  
maximilian.nolte@tu-darmstadt.de

Sebastian Schöps

Computational Electromagnetics  
Technische Universität Darmstadt  
Darmstadt, Germany  
sebastian.schoeps@tu-darmstadt.de

Riccardo Torchio

Department of Industrial Engineering  
Universita degli Studi di Padova  
Padova, Italy  
riccardo.torchio@unipd.it

**Abstract**—We discuss the advantages of a spline-based freeform shape optimization approach using the example of a multi-tapered coaxial balun connected to a spiral antenna. The underlying simulation model is given in terms of a recently proposed isogeometric integral equation formulation, which can be interpreted as a high-order generalization of the partial element equivalent circuit method. We demonstrate a significant improvement in the optimized design, i.e., a reduction in the magnitude of the scattering parameter over a wide frequency range.

**Index Terms**—Antenna, optimization, splines, boundary element method

## I. INTRODUCTION

In the design of electromagnetic components, the widely accepted computational alternative to a knowledge-based approach is algorithmic optimization. This topic is particularly well established in the design of antennas, see e.g., [1]. The space of design parameters that defines the shape of the component is usually categorized as geometric parameters (e.g., length, width), free form shapes (e.g., represented by splines), or topologies (including holes, etc.), Fig. 1. After the design parameters are chosen, they are varied algorithmically by an optimizer, which can be broadly classified as stochastic (e.g., particle swarm) or deterministic (e.g., gradient based), [2].

Traditionally, an appropriate parameterization of the geometry must be found, and the model must be repeatedly meshed to compute the changing properties using a numerical method. Meshing is potentially expensive and may require manual corrections, which hinders automatic approaches [3]. In addition, the resulting designs are limited by the choice of parameters. In contrast, freeform shape optimization greatly increases design freedom, for example, by allowing any geometric point to be moved or by acting on the underlying

computer aided design (CAD) representation. By following the paradigm of isogeometric analysis (IGA) [4], where the same CAD basis functions are used to represent the solution and the geometry, freeform shape optimization can be performed directly on the CAD model.

Furthermore, the combination of IE and IGA allows to use the boundary representation (B-rep) provided by most popular CAD software, eliminating the tedious step of volume meshing as currently proposed in [5]. Using this formulation, we are able to optimize the triple-tapered coaxial balun proposed and analyzed in [6] using a deterministic (derivative-free) optimization algorithm. Furthermore, the IE formulation is advantageous for open space problems, such as antenna radiation.

The rest of this paper is organized as follows. In Section II we discuss how the computational domain is given in terms of B-splines and non-uniform rational B-splines (NURBS). In Section III we explain the formulation and discretization. Then, in Section IV we describe the optimization procedure, we used to optimize the coaxial balun. Finally, we summarize the results in Section V.

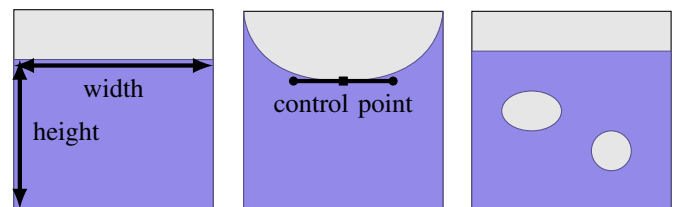


Fig. 1. Parameter (left), shape (middle) and topology optimization (right).

## II. BOUNDARY REPRESENTATION

In contemporary CAD software, the computational domain is frequently given by B-rep models in terms of NURBS [7]. The underlying basis functions are B-splines which can be defined using a  $p$ -open knot vector  $\Xi = [\xi_1, \dots, \xi_{k+p+1}] \in [0, 1]^{k+p+1}$ , where  $k$  denotes the number of control points. We can then define the basis functions for  $x \in (0, 1)$  and  $1 \leq i \leq k$  as

$$b_i^0(x) = \begin{cases} 1, & \text{if } \xi_i \leq x < \xi_{i+1}, \\ 0, & \text{otherwise,} \end{cases} \quad (1)$$

and for any positive polynomial degree  $p > 0$  via the recursive formula

$$b_i^p(x) = \frac{x - \xi_i}{\xi_{i+p} - \xi_i} b_i^{p-1}(x) + \frac{\xi_{i+p+1} - x}{\xi_{i+p+1} - \xi_{i+1}} b_{i+1}^{p-1}(x). \quad (2)$$

The B-splines  $b_i^p$  span a one-dimensional function space and for higher dimensions we can obtain corresponding spaces by tensor-product construction, [8]. An example of a one-dimensional spline with two-dimensional control points that produces a piece wise smooth curve with two kinks is shown in Fig. 2 with the corresponding knot vector and basis functions.

In applications, the computational domain is usually given by several NURBS patches, i.e.,

$$\Gamma = \bigcup_{n=1}^{N_\Gamma} \Gamma_n, \quad (3)$$

where the parameterization of each patch  $\Gamma_n$  is then given by a mapping from the two-dimensional reference domain  $(0, 1) \times (0, 1)$  to the computational domain, via

$$\Gamma_n(x, y) = \sum_{j_1=1}^{k_1} \sum_{j_2=1}^{k_2} \frac{\mathbf{p}_{j_1, j_2}^n b_{j_1}^{p_1}(x) b_{j_2}^{p_2}(y) w_{j_1, j_2}^n}{\sum_{i_1=1}^{k_1} \sum_{i_2=1}^{k_2} b_{i_1}^{p_1}(x) b_{i_2}^{p_2}(y) w_{i_1, i_2}^n}, \quad (4)$$

with three-dimensional control points  $\mathbf{p}_{j_1, j_2}^n$  and weights  $w_{i_1, i_2}^n$ . We assume that patches are conforming, i.e., adjacent patches share either exactly one vertex or one edge where the parameterizations coincide up to orientation.

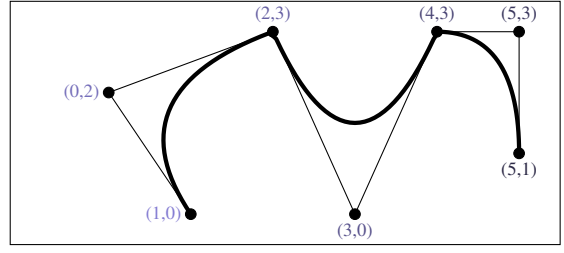
## III. INTEGRAL FORMULATION

Let the free space be denoted by  $\Omega$  and the perfectly electric conducting surface by  $\Gamma$  as defined in (3). The scattering problem is to compute for a given incident field  $\mathbf{E}_i$  the scattered field  $\mathbf{E}_s$  that satisfies

$$\begin{cases} \mathbf{curl} \mathbf{curl} \mathbf{E}_s - \kappa^2 \mathbf{E}_s = 0 & \text{in } \Omega, \\ \mathbf{E}_s \times \mathbf{n} = -\mathbf{E}_i \times \mathbf{n} & \text{on } \Gamma, \end{cases} \quad (5)$$

with the wave number  $\kappa = \omega \sqrt{\varepsilon \mu}$  defined in terms of angular frequency  $\omega$ , permittivity  $\varepsilon$  and permeability  $\mu$  and the normal vector  $\mathbf{n}$  on  $\Gamma$ . Furthermore,  $\mathbf{E}_s$  needs to fulfil the Silver-Müller radiation condition [9, p. 29]. A solution to (5) is given by the Stratton and Chu representation formula, cf., [10, Sec. 8.14]. We use the potential formulation

$$\mathbf{E}_s(\mathbf{x}) = -j\omega \mathbf{A}(\mathbf{x}) - \mathbf{grad} \varphi(\mathbf{x}), \quad \mathbf{x} \in \Omega, \quad (6)$$



$$\Xi = [0, 0, 0, 1/3, 1/3, 1/3, 2/3, 2/3, 2/3, 1, 1, 1]$$

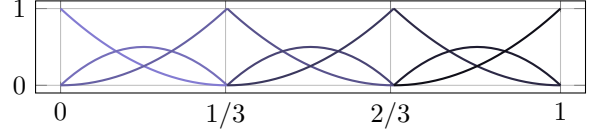


Fig. 2. An exemplary spline curve with kinks at  $x = 1/3$  and  $x = 2/3$ .

with the magnetic vector potential

$$\mathbf{A}(\mathbf{x}) = \mu \int_{\Gamma} \mathbf{j}(\mathbf{y}) g_{\kappa}(\mathbf{x}, \mathbf{y}) d\Gamma_{\mathbf{y}}, \quad (7)$$

and the electric scalar potential

$$\varphi(\mathbf{x}) = \frac{1}{\varepsilon} \int_{\Gamma} \varrho(\mathbf{y}) g_{\kappa}(\mathbf{x}, \mathbf{y}) d\Gamma_{\mathbf{y}}. \quad (8)$$

Where  $\mathbf{j}$  is the electric surface current,  $\varrho$  is the electric surface charge and

$$g_{\kappa}(\mathbf{x}, \mathbf{y}) = \frac{e^{-i\kappa|\mathbf{x}-\mathbf{y}|}}{4\pi|\mathbf{x}-\mathbf{y}|}, \quad (9)$$

denotes the homogeneous space Green's function. We employ an A-EFIE formulation from [11] with higher-order B-spline basis functions, for which a rigorous derivation can be found in [5]. The discretization in terms of the current  $\mathbf{j}$  and the potential  $\varphi$  leads to the linear system of equations

$$\begin{pmatrix} j\omega \mathbf{L} & \mathbf{G}^T \\ \mathbf{P} \mathbf{M}^{-1} \mathbf{G} & -j\omega \mathbf{M} \end{pmatrix} \begin{pmatrix} \mathbf{J} \\ \Phi \end{pmatrix} = \begin{pmatrix} \mathbf{v}_{\text{ex}} \\ \mathbf{0} \end{pmatrix}, \quad (10)$$

where  $\mathbf{J}$  and  $\Phi$  store the degrees of freedom of  $\mathbf{j}$  and  $\varphi$ , respectively. The matrix entries for the inductive and capacitive effects are computed as follows

$$\begin{aligned} L_{ij} &= \mu \int_{\Gamma} \int_{\Gamma} g_{\kappa}(\mathbf{x}, \mathbf{y}) \mathbf{v}_i \cdot \mathbf{v}_j d\Gamma_{\mathbf{y}} d\Gamma_{\mathbf{x}}, \\ P_{ij} &= \frac{1}{\varepsilon} \int_{\Gamma} \int_{\Gamma} g_{\kappa}(\mathbf{x}, \mathbf{y}) v_i v_j d\Gamma_{\mathbf{y}} d\Gamma_{\mathbf{x}}, \end{aligned}$$

where  $\mathbf{v}_i, \mathbf{v}_j$  and  $v_i, v_j$  are adequate vector- and scalar-valued tensor-product B-spline basis functions, respectively [5], [12]. The entries in the matrix blocks  $\mathbf{L}$  and  $\mathbf{P}$  in (10) contain singular integrals. We use the Duffy trick for the quadrature of these singular integrals [13]. For the non-singular integrals usual tensor-product Gauss-Legendre quadrature is applied [14]. The remaining matrix and vector entries are given by

$$G_{ij} = \int_{\Gamma} v_i \text{div } \mathbf{v}_j d\Gamma_{\mathbf{x}}, \quad M_{ij} = \int_{\Gamma} v_i v_j d\Gamma_{\mathbf{x}}$$

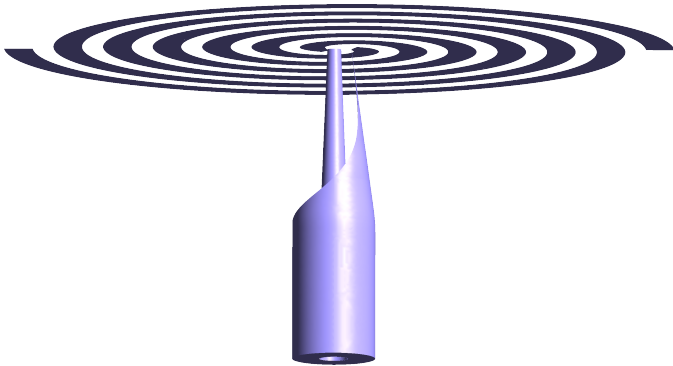


Fig. 3. Visualization of balun with attached spiral antenna with tapers based on the design of [6].

and

$$v_{\text{ex},i} = \int_{\Gamma} (\mathbf{E}_i \times \mathbf{n}_x) \cdot \mathbf{v}_i d\Gamma_x.$$

When using lowest-order spline basis functions, the resulting formulation is equivalent to the partial element equivalent circuit (PEEC) method [15]. Even in this case, unlike classical (‘orthogonal’) PEEC, we can still work with arbitrarily curved spline geometries. Nonetheless, impedance  $\mathbf{Z}(\omega)$ , admittance  $\mathbf{A}(\omega)$  and scattering matrices  $\mathbf{S}(\omega)$  can be computed from (10) as in the original circuit-like formulation, see [16, Section 2.8]. Therefore, we will refer to our approach as IGA PEEC.

Note, that all matrix entries and thus the solution of (10) as well as the scattering parameter depend on the geometry which is given by the control points and weights of the spline surfaces  $\Gamma_n$  in (4). By slight abuse of notation we denote all those dependencies by  $\mathbf{p}$  as in  $\mathbf{S}^{\mathbf{p}}(\omega)$  for the scattering parameter.

#### IV. OPTIMIZATION RESULTS

We use the integral formulation (10) to calculate the scattering parameters for the multi-tapered coaxial balun shown in Fig. 3. The software implementation is based on Bembel [17] and uses  $N_{\Gamma} = 271$  patches and  $N_{\text{dof}} = 2871$  degrees of freedom. The multipatch NURBS model can be found at [18]. It is motivated by the work of McParland et al., who proposed in [6] a new interesting design for a coaxial balun: the unbalanced port is a coaxial cable, whose outer conductor is cut open and gradually reduced to the second wire of the balanced port. It features a new triple-tapered design where the inner and outer conductor radius, as well as the opening angle are allowed to follow an arbitrary profile. The purpose of this structure is to convert signals between the differing ports, while also performing an impedance transformation [6]. One of their examples is the balun with a spiral antenna attached as shown in Fig. 3. Here, the quantity to optimize is the reflection loss over the frequency band of interest, quantified by the scattering parameter. McParland et al. optimize the design based on expert knowledge, i.e., using a combination of analytical computations, numerical simulation studies and

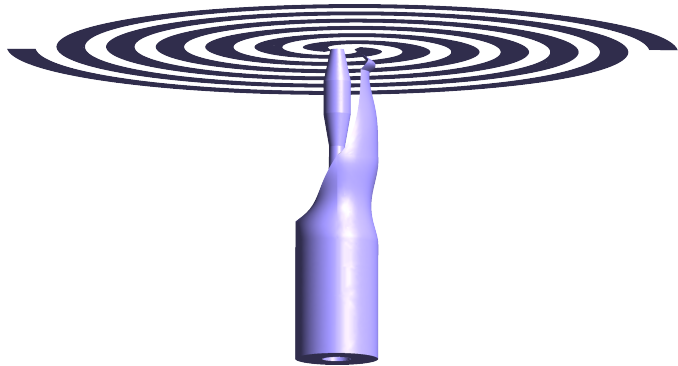


Fig. 4. Visualization of the optimized balun design.

measurements. Notably, they suggest that more complex profiles are possible and may lead to even better results.

We proceed to implement a freeform shape optimization process for the taper profiles. Let  $\mathbf{p}$  denote the subset of the control points ( $N_{\mathbf{p}} = 25$  points in total) defining the profiles, such that the overall geometry remains cylindrical. Furthermore, let  $\mathcal{P}$  be the admissible set of control points, such that for example intersections are avoided. We solve the optimization problem

$$\min_{\mathbf{p} \in \mathcal{P}} \left( \sum_{i=1}^{N_{\omega}} |S_{11}^{\mathbf{p}}(\omega_i)|^q \right)^{1/q} \quad (11)$$

where  $S_{11}^{\mathbf{p}}(\omega_i)$  is the scattering parameter (measuring the reflection at port 1) for the geometry resulting from control points  $\mathbf{p}$  at angular frequency  $\omega_i$ . The  $N_{\omega} = 21$  frequencies  $\omega_i$  are chosen as equidistant samples between 8 and 18 GHz, which corresponds to the frequency band of interest in [6]. The  $q = 8$  norm is chosen to ensure the minimization of the largest  $|S_{11}^{\mathbf{p}}(\omega_i)|$  values.

For the numerical optimization we employ the deterministic (derivative-free) bound optimization by quadratic approximation (BOBYQA) algorithm [19] implemented in the Python package Py-BOBYQA [20], [21]. We use the default parameters with global optimization and increased trust-region-radius start, end, and scaling-after-restart values (0.2, 0.01, 1.2) with which the optimizer stagnates after approx.  $N_{\text{iter}} = 80$  iterations. This process takes a few hours using significant parallelization.

The reflections measured by the magnitude of  $S_{11}(\omega)$  of the original design and the optimization results are visualized in Fig. 5. We observe a clear improvement, which can be quantified by a reduction of the goal function (11) by approx. 55 percent where we have used  $N_{\omega} = 200$  equidistant frequency samples. To verify the results, the CAD models of the original and the optimized design are simulated with FEKO [22]. Data export and import is straightforward since the geometry data is given in the form of NURBS and can therefore be easily exported in CAD file formats such as STEP or IGES. The simulation results from FEKO are in agreement

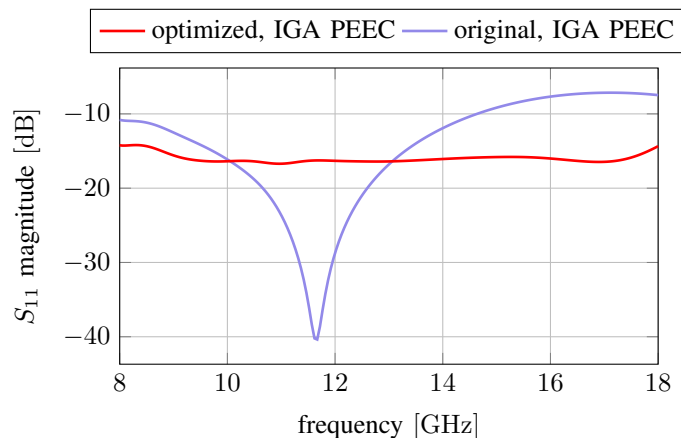


Fig. 5. Magnitudes of scattering parameter for original and optimized geometry using  $N_\omega = 200$  frequency samples.

with our results and show a similar level of improvement, which confirms the effectiveness of our optimization.

## V. CONCLUSION

This paper demonstrates the advantages of using spline-based freeform shape optimization in the design of high-frequency components using the example of a coaxial balun connected to a spiral antenna. By using an isogeometric integral equation method, the traditional, computationally expensive re-meshing steps during the optimization procedure can be effectively bypassed. This approach allows computation directly on CAD models, improving both geometric accuracy and computational efficiency in the optimization process. Future research may investigate the computation and exploitation of (higher) derivatives, see e.g., [23], [24], so that derivative-based optimization algorithms such as sequential quadratic programming (SQP) can be used, which are often more efficient [2].

## ACKNOWLEDGMENT

The authors thank Albert E. Ruehli for the many fruitful discussions regarding PEEC and the balun example. This work was supported in part by the Graduate School CE within the Centre for Computational Engineering at Technische Universität Darmstadt, by the German Research Foundation under Project 443179833, the DAAD in the Framework of Short-Term Grants under 57588366 and the Future Talent Guest Stay program of TU Darmstadt. Finally, the support of the LOEWE project 1450/23-04 via the Hessian Ministry of Science and Art and the Hessen-Agentur is acknowledged.

## REFERENCES

- [1] C. A. Balanis, *Antenna Theory: Analysis and Design*, 4th ed. Wiley, 2016.
- [2] J. Nocedal and S. J. Wright, *Numerical optimization*, 2nd ed., ser. Springer Series in Operations Research and Financial Engineering. Springer, 2006.

- [3] P. T. Boggs, A. Altshuler, A. R. Larzelere, E. J. Walsh, R. L. Clay, and M. F. Hardwick, "DART system analysis," Sandia National Laboratories, Technical Report SAND2005-4647, 2005.
- [4] J. A. Cottrell, T. J. R. Hughes, and Y. Bazilevs, *Isogeometric Analysis: Toward Integration of CAD and FEA*. Wiley, 2009.
- [5] M. Nolte, R. Torchio, S. Schöps, J. Dölz, F. Wolf, and A. E. Ruehli, "A low-frequency-stable higher-order spline-based integral equation method," Cornell University, Preprint arxiv:2401.10735, 2024.
- [6] K. P. McParland and M. S. Mirotznik, "Design and additive manufacture of multi-tapered coaxial baluns," *IEEE Trans. Compon. Packag. Manuf.*, vol. 12, no. 11, pp. 1806–1815, 2022.
- [7] L. Piegl and W. Tiller, *The NURBS Book*, 2nd ed. Springer, 1997.
- [8] T. J. R. Hughes, J. A. Cottrell, and Y. Bazilevs, "Isogeometric analysis: CAD, finite elements, NURBS, exact geometry and mesh refinement," *Comput. Meth. Appl. Mech. Eng.*, vol. 194, pp. 4135–4195, 2005.
- [9] S. Kurz and B. Auchmann, "Differential forms and boundary integral equations for Maxwell-type problems," in *Fast Boundary Element Methods in Engineering and Industrial Applications*, ser. Lecture Notes in Applied and Computational Mechanics, U. Langer, M. Schanz, O. Steinbach, and W. L. Wendland, Eds. Springer, 2012, no. 63, pp. 1–62.
- [10] J. A. Stratton, *Electromagnetic Theory*. IEEE Press, 1941.
- [11] Z. G. Qian and W. C. Chew, "An augmented electric field integral equation for high-speed interconnect analysis," *IEEE Trans. Antenn. Propag.*, vol. 50, no. 10, pp. 2658–2662, 2008.
- [12] A. Buffa, J. Dölz, S. Kurz, S. Schöps, R. Vázquez, and F. Wolf, "Multipatch approximation of the de Rham sequence and its traces in isogeometric analysis," *Numer. Math.*, vol. 144, no. 1, pp. 201–236, 06 2019, arxiv:1806.01062.
- [13] M. G. Duffy, "Quadrature over a pyramid or cube of integrands with a singularity at a vertex," *SIAM J. Numer. Anal.*, vol. 19, no. 6, pp. 1260–1262, 1982.
- [14] H. Harbrecht and R. Schneider, "Wavelet Galerkin Schemes for Boundary Integral Equations—Implementation and Quadrature," *SIAM J. Sci. Comput.*, vol. 27, no. 4, pp. 1347–1370, 2006.
- [15] A. E. Ruehli, "Equivalent circuit models for three-dimensional multi-conductor systems," *IEEE Trans. Microw. Theor. Tech.*, vol. 22, no. 3, pp. 216–221, 1974.
- [16] A. E. Ruehli, G. Antonini, and L. Jiang, *The Partial Element Equivalent Circuit Method for Electro-Magnetic and Circuit Problems*, 1st ed. John Wiley & Sons, 2017.
- [17] J. Dölz, H. Harbrecht, S. Kurz, M. Multerer, S. Schöps, and F. Wolf, "Bembel: The fast isogeometric boundary element C++ library for Laplace, Helmholtz, and electric wave equation," *Software X*, vol. 11, p. 100476, 04 2020, arxiv:1906.00785.
- [18] B. Balouchev, J. Dölz, M. Nolte, S. Sebastian, and R. Torchio, "Results of a iga-peec-based multi-tapered coaxial balun optimization," 2024. [Online]. Available: [https://github.com/temf/igapeec\\_balun\\_opt](https://github.com/temf/igapeec_balun_opt)
- [19] M. J. D. Powell, "The BOBYQA algorithm for bound constrained optimization without derivatives," Cambridge University, Technical Report DAMTP 2009/NA06, 08 2009.
- [20] C. Cartis, J. Fiala, B. Marteau, and L. Roberts, "Improving the flexibility and robustness of model-based derivative-free optimization solvers," *ACM Trans. Math. Software*, vol. 45, no. 3, pp. 1–41, 08 2019, arxiv:1804.00154.
- [21] C. Cartis, L. Roberts, and O. Sheridan-Methven, "Escaping local minima with local derivative-free methods: a numerical investigation," *Optimization*, vol. 71, no. 8, p. 2343–2373, Feb. 2021.
- [22] Altair, *Feko – User Guide*, Altair Engineering Inc., 04 2023. [Online]. Available: [https://help.altair.com/feko/pdf/Altair\\_Feko\\_User\\_Guide.pdf](https://help.altair.com/feko/pdf/Altair_Feko_User_Guide.pdf)
- [23] A. Ziegler, M. Merkel, P. Gangl, and S. Schöps, "On the computation of analytic sensitivities of eigenpairs in isogeometric analysis," *Comput. Meth. Appl. Mech. Eng.*, vol. 409, p. 115961, 05 2023, arxiv:2212.10347.
- [24] A. Ziegler, R. Hahn, V. Isensee, A. D. Nguyen, and S. Schöps, "Gradient-based eigenvalue optimization for electromagnetic cavities with built-in mode matching," *IET Sci. Meas. Tech.*, 10 2023, arxiv:2310.15751.